The hydrogen bonded polymer structures of $[\{Mn(2\text{-}mbiH)_2 \cdot TMEDA\} \cdot A\text{–}A]_\infty$ [2-mbiH$_2$ = 2-mercaptobenzimidazole; A–A = TMEDA ($Me_2NCH_2CH_2NMe_2$) or DABCO ($N\{CH_2CH_2\}_3N$)]

Michael A. Beswick, Marta E. G. Mosquera, Julie S. Palmer, Paul R. Raithby and Dominic S. Wright*

Chemistry Department, University of Cambridge, Lensfield Road, Cambridge, UK CB2 1EW

Received (in Cambridge, UK) 18th November 1998, Accepted 30th July 1999

The reaction of [$MnCp_2$] with 2-mbiH$_2$ (1 : 2 equiv.) in the presence of TMEDA gives $[\{Mn(2\text{-}mbiH)_2 \cdot TMEDA\} \cdot TMEDA]_\infty$ **1**. A similar reaction employing TMEDA and DABCO (1 : 1 equiv.) yields $[\{Mn(2\text{-}mbiH)_2 \cdot TMEDA\} \cdot DABCO]_\infty$ **2**. In the crystal, both complexes adopt similar polymeric structures in which the bifunctional [$Mn(2\text{-}mbiH)_2 \cdot TMEDA$] units are associated by hydrogen bonds to lattice-bound TMEDA or DABCO ligands. The structural motif adopted by both complexes can be regarded as resulting from a fusion of separate helical elements.

Introduction

Previously it has been shown that acid/base or nucleophilic substitution reactions of Group 14 metallocenes (ECp_2; E = Sn, Pb) can be employed in the synthesis of a variety of complexes.[1] However, possibly reflecting the commonly perceived low polarity of Cp–M interactions in the metallocenes of transition metals, the similar use of these species as soluble sources of low-oxidation state metals has been investigated far less extensively. Instead, reactions of tris(trimethyl)silylamido complexes $[M\{N(SiMe_3)_3\}_x]$ (containing more polar metal–N bonds) with organic acids or nucleophiles have been frequently employed to access a range of organometallic and metallo-organic compounds.[2] The use of metallocene derivatives in this context is clearly most viable for transition elements on the right-hand side of the series since contraction of the d-orbitals diminishes their involvement in Cp–metal bonding and, in some respects, the bonding approaches that found in p block metallocenes. In earlier work it was shown that displacement of the Cp ligands of manganocene ($MnCp_2$) by nucleophiles is a highly effective route to a range of organometallic complexes containing Mn(II).[3] The Cp ligands of metallocenes of Group 11 metals [$MCp \cdot PR_3$; M = Cu, Ag] prove to be similarly labile.[4] We present here a study of the reaction of $MnCp_2$ with 2-mercaptobenzimidazole [2-mbiH$_2$ = $C_6H_4N{=}C(SH)NH$] which illustrates that this metallocene can be used as a readily accessible organometallic base. Structural studies of the two complexes $[\{Mn(2\text{-}mbiH)_2 \cdot TMEDA\} \cdot TMEDA]_\infty$ **1** [TMEDA = $(Me_2NCH_2)_2$] and $[\{Mn(2\text{-}mbiH)_2 \cdot TMEDA\} \cdot DABCO]_\infty$ **2** [DABCO = $N(CH_2CH_2)_3N$] reveal that both complexes adopt related polymeric structures by virtue of strong hydrogen bonding between the metal bonded 2-mbiH groups and the lattice bound bidentate nitrogen donor ligands present.

Results and discussion

One interest of ours has been the use of halide-free routes to a variety of main group and transition metal organometallic and metallo-organic compounds. In this context we have explored the use of stannocene ($SnCp_2$) as a reagent to a range of Sn(II) complexes,[5] such as stannates (containing SnR_3^- anions) and imido Sn complexes (of the type $[SnNR]_4$).[6] The studies involving manganocene ($MnCp_2$) presented here represent our first efforts to explore the possible similarity between this species and its Sn(II) relative. Although displacement of the Cp ligands from $MnCp_2$ has been well established,[3] to our knowledge acid/base reactions have not so far been employed. Reactions of $MnCp_2$ with 2-mercaptobenzimidazole were explored since this reasonably acidic organic acid represents a good probe. Although complexes of Mn(II) and this ligand have not been reported previously, various complexes containing similar N,S-chelating ligands have been structurally characterised.[7]

$[\{Mn(2\text{-}mbiH)_2 \cdot TMEDA\} \cdot TMEDA]_\infty$ **1** is best prepared by the reaction of $MnCp_2$ with 2-mbiH$_2$ (1 : 2 equivalents) using an excess of TMEDA (>2 equivalents) (Scheme 1). In the light of the later structural characterisation of **1** by X-ray crystallography which shows that the extra molecule of TMEDA is involved in associating the [$Mn(2\text{-}mbiH)_2 \cdot TMEDA$] monomer units into a polymeric hydrogen bonded structure, we decided to investigate the structural effects of introducing another bidentate Lewis base into this system. Accordingly, the reaction of $MnCp_2$ with 2-mbiH$_2$ (1 : 2 equivalents) was performed in the presence of TMEDA and DABCO (1 : 1 equivalents) (Scheme 1). The choice of DABCO as the hydrogen bonding spacer in this system was governed by its greater geometric rigidity than TMEDA (which it was assumed would have the maximum effect on the supramolecular architecture of the resulting polymer) and by the fact that as a non-chelating ligand competition with TMEDA for metal coordination should be minimised for thermodynamic/kinetic reasons (*i.e.*, the chelate effect). The isolated complex from this reaction was $[\{Mn(2\text{-}mbiH)_2 \cdot TMEDA\} \cdot DABCO]_\infty$ **2**.

$$MnCp_2 + 2(2\text{-}mbiH_2) \xrightarrow{\text{TMEDA/L (1:1)}} [Mn(2\text{-}mbiH)_2 \cdot TMEDA] \cdot L + 2CpH$$

L = TMEDA **1**, DABCO **2**

Scheme 1

The characterisation of **1** and **2** was made primarily by elemental analysis (C, H and N) and IR spectroscopy since their paramagnetic nature rendered even standard NMR investigations unsatisfactory. The crystal structures of both complexes were obtained. Details of the data collections and refinements are given in Table 1. Table 2 lists key bond lengths and angles found in complex **1**. Whereas the structure of **1** was obtained at 180 K, for complex **2** shock cooling to this temperature resulted in the crystals shattering due to a phase change occurring at *ca.* 200 K. The structure of the high-temperature monoclinic phase (**2a**) was initially obtained at 210 K prior to gradual cooling to 180 K which preserved the integrity of the crystal, the data on the low-temperature triclinic phase (**2b**) then being obtained. Repeated cycles of cooling to 180 K and heating to 210 K (with redetermination of the cell dimensions) showed that the phase change is fully reversible. Table 3 lists key bond lengths and angles for these phases.

Complex **1** is composed of alternating enantiomers of [Mn(2-mbiH)$_2$·TMEDA] (generated by the crystallographic symmetry of the centrosymmetric lattice) which are linked together by hydrogen bonding to lattice-bound TMEDA molecules into polymeric strands (Fig. 1). There are no significant intermolecular interactions occurring between these strands. Within this polymeric array the [Mn(2-mbiH)$_2$·TMEDA] units therefore act as bifunctional hydrogen bond donors (D–D) and the TMEDA molecules behave as bifunctional hydrogen bond acceptors (A–A).[8] The nature of the polymer is fundamentally a consequence of the pseudo-octahedral geometry of the constituent [Mn(2-mbiH)$_2$·TMEDA] units. The coordination of the Mn^{2+} cations by TMEDA [Mn(1A)–N(5AA,6AA) mean 2.36 Å] and their N,S-chelation by two 2-mbiH ligands [Mn(1A)–N(1AA,3AA) mean 2.20 Å, Mn(1A)–S(1AA,2AA) mean 2.69 Å] results in a highly distorted metal geometry in which the S centres of the 2-mbiH ligands are orientated *trans* to each other S(1AA)–Mn(1A)–S(2AA) 151.33(6)°]. The resulting 'concave' 2-mbiH ligand surface leads directly to an approximately anti-parallel alignment of the N–H groups. The hydrogen bonding of the N lone pairs of the TMEDA ligands to the N–H functions of a neighbouring enantiomer of [Mn(2-mbiH)$_2$·TMEDA] results in the alignment of the planes of the associated 2-mbiH ligands parallel to each other (the TMEDA N–N vectors being essentially perpendicular to the 2-mbiH planes). Judging from the shortness of the N(–H)···N interactions present in **1** these hydrogen bonds are strong [N(7AA)···N(4AA) 2.871(4) {H···N(7AA) 1.992 Å}, N(7AA)···H–N(4AA) 177.9° and N(2AA)···N(8AA) 2.860(4) {H···N(8AA) 1.933 Å}, N(8AA)···H–N(2AA) 166.8°; *cf.* sum of van der Waals' radii for N···N of *ca.* 3.00 Å[9] and the normal range observed of 2.94–3.15 Å[10]]. A search of the Cambridge Structural Database reveals that there have been no examples of N–H···N hydrogen bonds occurring between fragments of the type found in **1** and neutral secondary amine fragments reported.[11] Normally proton transfer to the secondary amines occurs under these circumstances, with the N···N distances being in the range 2.636–2.946 Å in these species.[12] The location of the H atoms in the difference map involved in the N–H···N interactions confirms that the correct formulation of **1** is [{Mn(2-mbiH)$_2$·TMEDA}·TMEDA]$_\infty$ rather than [{Mn(2-mbi)$_2$·TMEDA}$^{2-}${TMEDAH$_2$}$^{2+}$]$_\infty$. One implication of the strength of these interactions is that the Mn^{2+} ion is able to exert a significant electron withdrawing influence over the 2-mbiH ligand system (an effect which will increase the polarisation of the N–H bond).

The structures of the high-temperature and low-temperature phases of **2** (**2a** and **2b** respectively) are identical

Table 1 Crystal data for [{Mn(2-mbiH)$_2$·TMEDA}·TMEDA] **1** and [{Mn(2-mbiH)$_2$·TMEDA}·DABCO] (high-temperature phase **2a**, low-temperature phase **2b**)

	1 $C_{26}H_{42}MnN_8S_2$	**2a** $C_{26}H_{38}MnN_8S_2$	**2b** $C_{26}H_{38}MnN_8S_2$
M	585.74	581.70	581.70
T/K	180(2)	210(2)	180(2)
Crystal system	Triclinic	Monoclinic	Triclinic
Space group	$P\bar{1}$	$C2/c$	$P\bar{1}$
a/Å	11.851(4)	20.084(5)	20.032(6)
b/Å	18.442(6)	8.384(5)	21.966(6)
c/Å	7.695(2)	18.339(5)	16.522(5)
α/°	101.71(2)	–	112.11(4)
β/°	109.06(1)	107.08(4)	113.73(4)
γ/°	78.18(2)	–	94.26(4)
U/Å^3	1538.9(8)	2952(2)	5944(3)
Z	2	4	8
μ/mm^{-1}	0.593	0.618	0.614
Total reflections	7669	4886	22 931
Independent reflections (R_{int})	4885(0.073)	2575(0.042)	15 828(0.073)
R indices [$F > 4\sigma(F)$]	$R1 = 0.066$, $wR2 = 0.112$	$R1 = 0.043$, $wR2 = 0.084$	$R1 = 0.130$, $wR2 = 0.361$
R indices (all data)	$R1 = 0.130$, $wR2 = 0.132$	$R1 = 0.070$, $wR2 = 0.092$	$R1 = 0.219$, $wR2 = 0.403$

Table 2 Selected bond lengths (Å) and angles (°) for [{Mn(2-mbiH)$_2$·TMEDA}·TMEDA]$_\infty$ **1**

Mn(1A)–N(1AA)	2.188(4)	Mn(1A)–S(2AA)	2.692(2)
Mn(1A)–N(3AA)	2.203(5)	Mn(1A)–N(6AA)	2.350(5)
Mn(1A)–N(5AA)	2.367(4)	Mn(1A)–S(1AA)	2.690(2)
N(1AA)–Mn(1A)–S(1AA)	64.7(1)	N(5AA)–Mn(1A)–N(6AA)	77.1(2)
N(3AA)–Mn(1A)–S(2AA)	65.0(1)	N(1AA)–Mn(1A)–N(3AA)	111.7(2)
S(1AA)–Mn(1A)–S(2AA)	151.33(6)		
Hydrogen bonding			
N(2AA)(–H)···N(8AA)	2.860(4) (1.993)	N(4AA)(–H)···N(7AA)	2.871(4) (1.992)
N(2AA)–H···N(8AA)	166.8	N(4AA)–H···N(7AA)	177.9

Symmetry transformations used to generate equivalent atoms: A $-x+1, -y, -z+1$; B $-x+2, -y+1, -z$.

Table 3 Selected bond lengths (Å) and angles (°) for $[\{Mn(2\text{-}mbiH)_2 \cdot TMEDA\} \cdot DABCO]_\infty$ **2** for the α phase (210 K, **2a**) and β phase (180 K, **2b**)

α Phase[a]			
Mn(1)–N(2)	2.176(3)	Mn(1)–S(1)	2.714(2)
Mn(1)–N(3)	2.313(3)	N(4)(–H)···N(1)	2.884(4) (2.14)
N(2)–Mn(1)–S(3)	64.97(5)	N(3)–Mn(1)–N(3a)	78.9(2)
S(1)–Mn(1)–S(1a)	159.71(5)	N(2)–Mn(1)–N(2a)	105.0(1)
β Phase			
Molecule 1			
Mn(11)–N(41)	2.14(1)	Mn(11)–N(61)	2.35(1)
Mn(11)–N(11)	2.19(1)	Mn(11)–S(21)	2.739(6)
Mn(11)–N(51)	2.24(2)	Mn(11)–S(11)	2.779(6)
N(41)–Mn(11)–S(21)	63.4(4)	N(51)–Mn(11)–N(61)	76.6(5)
N(11)–Mn(11)–S(11)	65.1(4)	N(11)–Mn(11)–N(41)	103.3(5)
S(11)–Mn(11)–S(21)	157.7(2)		
Molecule 2			
Mn(12)–N(42)	2.20(1)	Mn(12)–N(62)	2.27(2)
Mn(12)–N(12)	2.17(1)	Mn(12)–S(22)	2.775(6)
Mn(12)–N(52)	2.32(1)	Mn(12)–S(12)	2.694(6)
N(12)–Mn(12)–S(12)	64.0(4)	N(52)–Mn(12)–N(62)	81.0(5)
N(42)–Mn(12)–S(22)	65.9(4)	N(12)–Mn(12)–N(42)	104.7(5)
S(12)–Mn(12)–S(22)	156.3(5)		
Molecule 3			
Mn(13)–N(43)	2.16(1)	Mn(13)–N(63)	2.29(1)
Mn(13)–N(13)	2.20(1)	Mn(13)–S(13)	2.663(6)
Mn(13)–N(53)	2.31(1)	Mn(13)–S(23)	2.726(6)
N(13)–Mn(13)–S(13)	66.6(4)	N(53)–Mn(13)–N(63)	74.4(5)
N(43)–Mn(13)–S(23)	64.0(4)	N(13)–Mn(13)–N(43)	107.1(5)
S(13)–Mn(13)–S(23)	155.9(2)		
Molecule 4			
Mn(14)–N(44)	2.22(1)	Mn(14)–N(64)	2.31(1)
Mn(14)–N(14)	2.20(1)	Mn(14)–S(14)	2.689(6)
Mn(14)–N(54)	2.40(1)	Mn(14)–S(24)	2.676(6)
N(14)–Mn(14)–S(14)	64.5(4)	N(54)–Mn(14)–N(64)	81.8(5)
N(44)–Mn(14)–S(24)	66.4(4)	N(14)–Mn(14)–N(44)	106.4(5)
S(14)–Mn(14)–S(24)	156.1(2)		
Hydrogen bonding			
N(21)(–H)···N(85)	2.855(4) (2.122)[b]	N(22)(–H)···N(76)	2.879(4) (2.101)[c]
N(31)(–H)···N(77)	2.900(4) (2.232)[b]	N(32)(–H)···N(88)	2.866(4) (2.100)[c]
N(23)(–H)···N(75)	2.840(4) (2.056)[b]	N(24)(–H)···N(86)	2.916(4) (2.045)[c]
N(33)(–H)···N(87)	2.964(4) (2.063)[b]	N(34)(–H)···N(78)	2.830(4) (2.087)[c]
N(21)–H···N(85)	146.2[b]	N(22)–H···N(76)	144.5[c]
N(31)–H···N(77)	132.5[b]	N(32)–H···N(88)	141.2[c]
N(23)–H···N(75)	155.4[b]	N(24)–H···N(86)	170.4[c]
N(33)–H···N(87)	151.2[b]	N(34)–H···N(78)	141.6[c]

[a] Symmetry transformations used to generate equivalent atoms: a $-x, y, -z + 3/2$; b $-x + 1/2, -y + 3/2, -z + 2$. [b] Found in one independent polymer strand. [c] Found in the other independent polymer strand.

in terms of their supramolecular architectures. The connectivity of **2b** is shown in Fig. 2. Both phases are composed of infinite polymeric strands in which enantiomeric molecules of $[Mn(2\text{-}mbiH)_2 \cdot TMEDA]$ are associated by hydrogen bonding to lattice-bound DABCO ligands (an ···A–A···D–D··· structural motif which is similar to that observed in **1**). The most obvious difference between these two phases is that the two-fold disorder of the DABCO ligand in **2a** is resolved in the low-temperature structure. In addition, in contrast to **2a** whose polymeric structure is constructed from only one crystallographically independent $[Mn(2\text{-}mbiH)_2 \cdot TMEDA]$ unit (its enantiomer being generated by symmetry), **2b** is composed of four crystallographically independent molecular units forming two strands. The two independent polymeric strands in **2b** result from the incorporation of the enantiomeric pairs of $[Mn(2\text{-}mbiH)_2 \cdot TMEDA]$ [molecules 1 and 3, and molecules 2 and 4 (see Table 3)] into separate chains. Although the $[Mn(2\text{-}mbiH)_2 \cdot TMEDA]$ molecular units of **2a** and **2b** are similar to those found in **1**, there is a noticeable expansion in the S–Mn–S angles in these species [159.71(5) in **2a** and mean 156.5° in **2b**; *cf.* 151.33(6)° in **1**] which may stem from the strain induced within this structure by the incorporation of the more rigid ('linear') DABCO spacer ligand. In addition to the N–H···N hydrogen bonds in **2a** and **2b**, there are further close C–H···S contacts made within and between individual polymer strands in both of the phases. Most noteworthy are the C–H···S interactions made between alternate $[Mn(2\text{-}mbiH)_2 \cdot TMEDA]$ units of each polymer strand and neighbouring, parallel polymer chains (2.985 Å in **2a** and in the range 2.730–2.911 Å in **2b**; sum of van der Waals' radii for H and S is 3.05 Å[7]), as shown in Fig. 2b. Although the H-atoms of the N–H···N bridges of **2a** could not be located in the final difference map, these were located in the structure of **2b** (illustrating, as in the case of **1**, that the protons reside on 2-mbi groups of the neutral Mn units). The N(–H)···N bond lengths within the N–H···DABCO···H–N bridges of **2a** and **2b** are nearly identical within crystallographic error [N(1)···N(4) 2.884(4) Å in **2a** and range 2.830(4)–2.916(4) Å in **2b**]. However, in each of the polymer chains of **2b** two distinct types of N–H···(DABCO)···H–N bridges are found. The net result of these (occurring alternately along the polymer chain) is that there is an alternate long (*ca.* 14.61 Å) and short (*ca.*

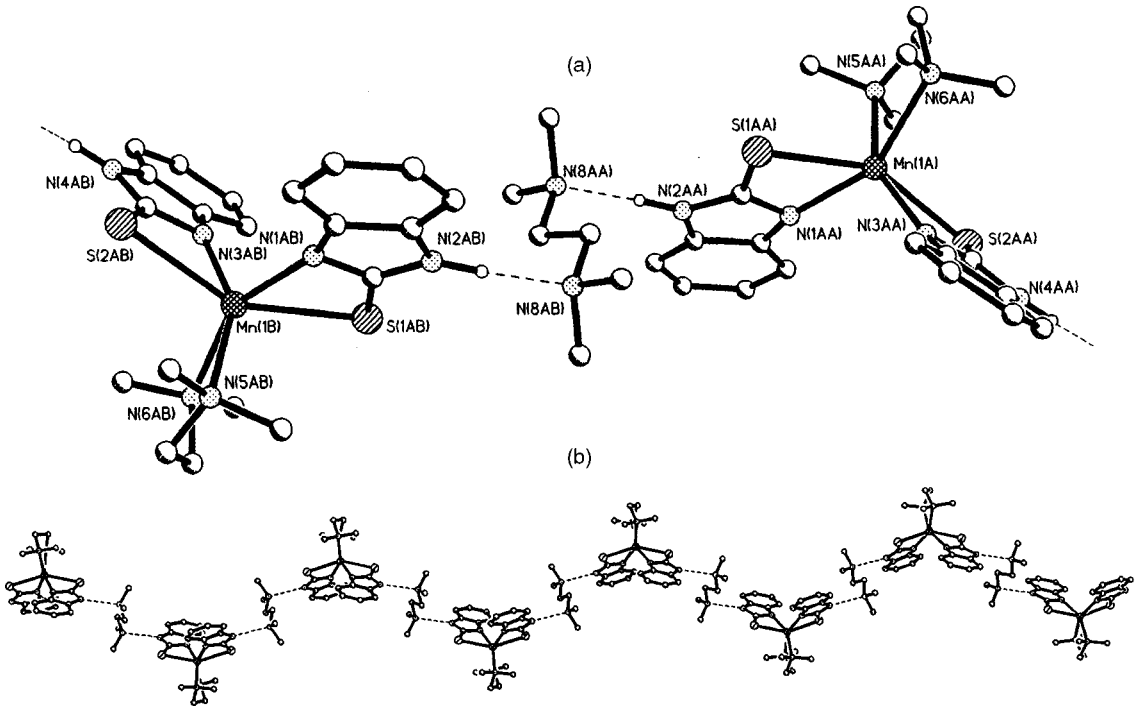

Fig. 1 Structure and connectivity of complex **1**.

14.30 Å) Mn···Mn spacing between the [Mn(2-mbiH)$_2$·TMEDA] units of the polymer backbones [*cf.* the equal spacing of Mn centres in **2a** (*ca.* 14.38 Å)].

In the past few decades the control of molecular assembly using supramolecular interactions in organic compounds has become a major area of research.[13] Mingos and co-workers have made great advances in the extension of these principles to transition metal complexes containing ligands which possess complementary hydrogen bond donor (N–H, OH) and acceptor sites (N, C=O).[14] Metal ions within these systems can act simply in a coordinative sense, providing a rigid framework for hydrogen bonding of the peripheral metal-bonded ligands, or the metal ions may have an additional electronic influence. Extensive studies by these workers (largely on Pt Group metals) have revealed that a wealth of supramolecular architectures can be in-built into oligomeric and extended lattices by incorporating metal-bonded ligands bearing specific double and triple hydrogen bonding functionalities.[14] The studies presented here represent a simpler (yet nonetheless related) aspect of this area in which the hydrogen bond donor functionality is confined to the metal fragment ([Mn(2-mbiH)$_2$·TMEDA]; D–D) and the hydrogen bond acceptor functionality is located solely on the spacer (TMEDA or DABCO; A–A). As such, the current study can be related to a recent investigation involving crystal engineering of complexes containing $[Ni\{tsc\}_2]^{2+}$ cations [tsc = thiosemicarbazide $\{(NH_2)NHC(NH_2)=S\}$] and the dicarboxylate anions [1,4-$(CO_2)_2C_6H_4]^{2-}$ and $[(CO_2)CH=CH(CO_2)]^{2-}$ in which major structural modification of the double hydrogen bonded ribbon structures results from the incorporation of the more rigid [1,4-$(CO_2)_2C_6H_4]^{2-}$ dianion (the latter adopt similar structures to those of **1** and **2** in the solid state).[15] The key difference in the structures of **1** and **2** is the presence of neutral metal and spacer units possessing hydrogen bonding capabilities. The effect of changing the flexible TMEDA ligand in **1** for the rigid DABCO spacer in **2** is to promote the alignment of the N–H functional groups of the 2-mbiH ligands in adjacent [Mn(2-mbiH)$_2$·TMEDA] units of the polymers of **2**. Overall, the connectivities and the nature of the polymer formed are the same in both complexes, the only significant difference being the non-linearity of the spacer in **1** which gives a 'kinked' appearance to the polymer strands (Fig. 3a). The polymer chains of **1** and **2** can be seen to represent an alternative to aggregation into a helical structure (another seemingly viable mode of association available to these species which has been observed in the structure of the hydrogen bonded Sb(III) complex $[Sb\{(NPr^i)_2CHNHPr^i\}\{(Pr^iN)_2CNPr^i\}]_\infty$ [16,17]). Strands of **1** and **2** (shown schematically in Fig. 3a and 3b, respectively) are composed of alternating right-hand and left-hand forms of the [Mn(2-mbiH)$_2$·TMEDA] units. The alternative would be to aggregate the units into separate α and β helices composed exclusively of each enantiomer. In this respect, the supramolecular structures of both complexes can be described as 'pseudo-helical' (a fusion of the α and β helical elements).

$$MnCp_2 + REHLi \rightarrow 1/n[MnER]_n + [CpLi] + CpH$$

Scheme 2

In summary, we have shown that $MnCp_2$ is a useful starting material in the preparation of metallo-organic derivatives of Mn(II) and a good alternative to (for example) $[Mn\{N(SiMe_3)_2\}_2]$ which has been used for the same purpose in previous studies. The latter is far more difficult to prepare and handle than the Cp derivative. In itself this could be viewed as only a minor technical advance. However, bearing in mind that the Cp groups of $MnCp_2$ are also susceptible to nucleophilic substitution the reactions of $MnCp_2$ with REHLi (E = N, P) are a promising way forward in the synthesis of Mn(II) imido and phosphinidine complexes (combining nucleophilic substitution of Cp^-, followed by elimination of CpH in a similar way to that observed for $SnCp_2$) (Scheme 2). The main focus of this paper has been the supramolecular structures of two complexes $[\{Mn(2\text{-}mbiH)_2\cdot TMEDA\}\cdot A\text{–}A]_\infty$ [A–A = TMEDA **1**, DABCO **2**] resulting from reactions of $MnCp_2$ with 2-mbiH$_2$. Strong hydrogen bonding occurs between the 'concave' bidentate hydrogen bond donor metal units and the bidentate hydrogen bond acceptor spacers in these systems.

Experimental

All reactions were carried out under an atmosphere of argon using standard inert atmosphere techniques. $MnCp_2$ was pre-

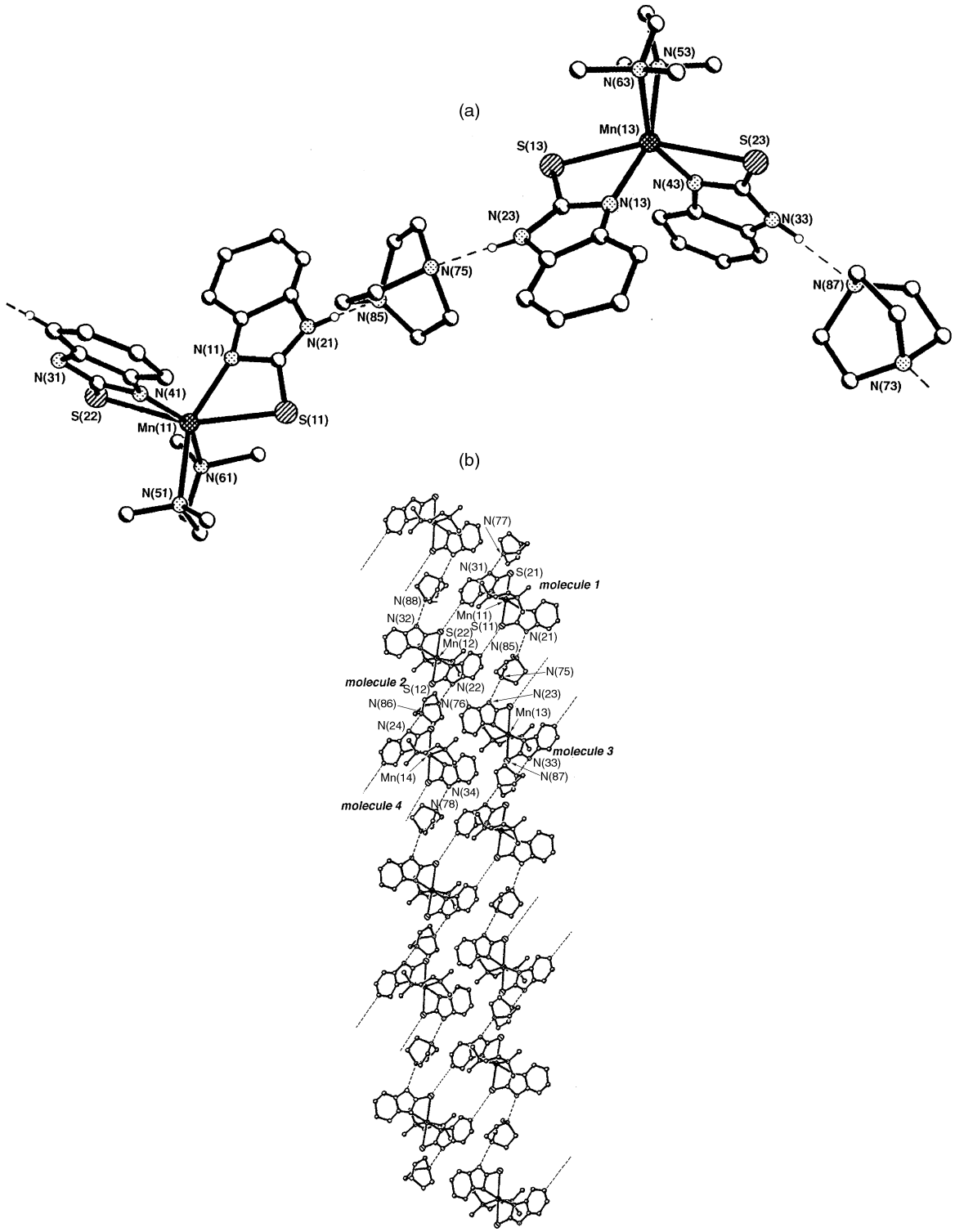

Fig. 2 (a) Structure and connectivity of **2b**, (b) two parallel strands of the polymer showing the inter-strand C–H···S interactions. The structure of **2a** is similar in its overall arrangement.

pared in a similar manner to that described in the literature[18] by the reaction of NaCp with $MnCl_2$ in thf, the product being purified by sublimation under vacuum. Tetrahydrofuran was dried by distillation over K–Na and TMEDA was used as supplied after drying with molecular sieve (13X). DABCO and 2-mbiH_2 were used as supplied (Aldrich).

Synthesis of 1

To a solution of $MnCp_2$ (2.78 g, 15 mmol) in thf (80 ml) and TMEDA (8.0 ml, 53 mmol) at −78 °C was added 2-mbiH_2 (4.51 g, 30 mmol) in thf (40 ml). The mixture was stirred for 30 min prior to filtration, a dark red-brown solution being produced. Reduction of the filtrate (to *ca.* 70 ml) gave a colourless precipitate which was heated back into solution. Storage at −15 °C (24 h) gave a crop of colourless blocks of **1**. Yield 2.95 g (34%); decomp. >330 °C; IR (Nujol), ν_{max}/cm^{-1} 3412, 3183 (br, N–H str.), other bands at 1296(m), 1268(m), 1022(m), 794(m), 745(s), 722(s); ^1H NMR (+25 °C, CD_2Cl_2, 250 MHz), uninformative. Calc. for $[\{Mn(2\text{-mbi}H)_2 \cdot TMEDA\} \cdot TMEDA]_\infty$: C 53.3, H 7.2, N, 19.1. Found: C 52.8, H 7.3, N 18.8%.

Synthesis of 2

To a solution of $MnCp_2$ (0.28 g, 1.5 mmol) in thf (20 ml) at −78 °C was added 2-mbiH_2 (0.45 g, 3.0 mmol). TMEDA (0.23

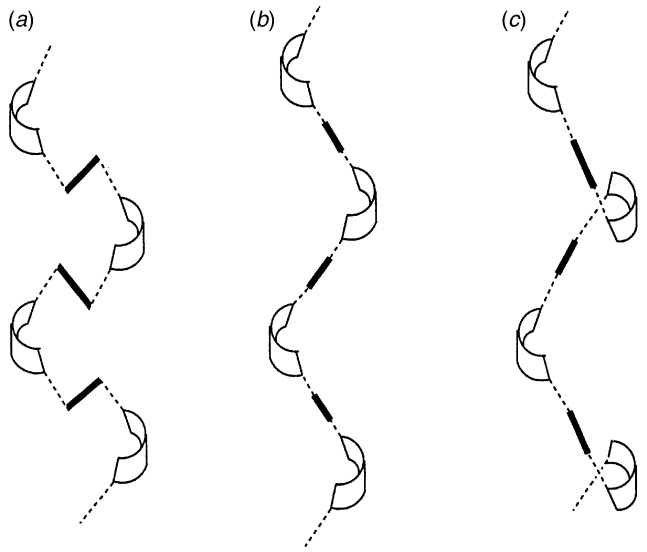

Fig. 3 Schematic representations of the pseudo-helical polymer structures of **1** and **2** [(a) and (b) respectively], and a potential helical arrangement (c).

ml, 1.5 mmol) was added and the mixture was stirred (30 min) before allowing the reaction to warm to room temperature. The mixture was cooled to −78 °C and DABCO (0.17 g, 1.5 mmol) was added. The mixture was stirred (30 min) and allowed to warm to room temperature, whereupon it was brought to reflux briefly. A beige suspension resulted which was filtered off to give an orange solution. Reduction of the filtrate (to *ca.* 10 ml) gave a white precipitate which was dissolved by the addition of thf (15 ml). Storage at −15 °C (1.5 h) gave a crop of colourless needles of **2** (crystals suitable for X-ray analysis were grown by storage at room temperature for 72 h). Yield 0.27 g (16%); decomp. to brown solid >200 °C; IR (Nujol), ν_{max}/cm^{-1} (no N–H observed above 3000 cm^{-1}) 1294(s), 1268(s), 1052(br, m), 792(m), 748(s), 722(m); ^1H NMR (+25 °C, CD_2Cl_2, 250 MHz), δ 6.56 (s), 6.47 (s, aryl C–H of 2-mbi group), 2.98 (s, DABCO), 1.63 (s, TMEDA) (accurate integrals could not be obtained). Calc. for $[\{Mn(2\text{-mbi}\mathbf{H})_2 \cdot TMEDA\} \cdot DABCO]_\infty$: C 53.7, H 6.5, N, 18.6. Found: C 53.7, H 6.6, N 19.3%.

Crystal structure determinations of 1, 2a and 2b

Suitable crystals of **1** and **2** were mounted on glass fibres, directly from solution, using perfluoropolyether oil which freezes at reduced temperatures[19] and holds the crystal static in the X-ray beam. Data for **1** were recorded on a Stoe four-circle diffractometer using ω–θ scans. Data for **2a** and **2b** were measured on the same crystal with a Rigaku R-AXIS-IIC image plate system. In each case, two sets of frames were collected to ensure a complete data set. The program PROCESS[20] was used to process and reduce the data, and to measure the cell dimensions. The data for **2a** were measured *before* cooling the crystal slowly to 180 K and measuring the data for **2b** (attempts to cool more rapidly destroyed other crystals). Despite the slow cooling, the data crystal did suffer during the phase transition: the data for **2b** are relatively poor (see Table 1) compared to that for **2a**. All instruments were equipped with an Oxford cryostream cooling device. For the structures of **1** and **2a** semi-empirical absorption corrections based on ψ scans were applied, while for **2b** the absorption correction was derived from interframe scaling. The structures were solved by direct methods and by subsequent Fourier difference syntheses[21] and were refined by full matrix least squares on F^2.[22] For **1** and **2a** the ordered non-hydrogen atoms were refined with anisotropic displacement parameters. In **2a** the disordered DABCO molecule was refined with partial occupancies over two sites. Structure **2b** is poorly resolved and is probably extensively disordered. In this case the Mn and S atoms only were refined with anisotropic displacement parameters: the C and N atoms were assigned common isotropic thermal factors and many distance constraints were included in the refinement, a strategy which reduced the total number of parameters to 545. The high *R*-factor (Table 1) reflects these problems. In the structures of **1a** and **2b** the 2-mbiH H-atom was located in the electron density difference maps, while in all three structures the remaining H-atoms were placed in idealised positions and allowed to ride on the relevant C atom, with isotropic displacement parameters set 1.5 times that of the C atom for the methyl groups and 1.2 times that for the other H-atoms. For each structure, in the final cycles of the refinement, a weighting scheme of $w = 1/[\sigma^2(F_0)^2 + (xP)^2 + yP]$ where $P = (F_0^2 + 2F_0^2)/3$ was introduced which resulted in a relatively flat analysis of variance.

CCDC reference number 440/134. See http://www.rsc.org/suppdata/nj/1999/1033/ for crystallographic files in .cif format.

Acknowledgements

We gratefully acknowledge the EPSRC (J.S.P.), the Leverhulme Trust (M.A.B.), the Royal Society (P.R.R., D.S.W.) and the E.U. (M.E.G.M) for financial support. We also thank Dr J. E. Davies (Cambridge) for collecting the X-ray data for **2a** and **2b** and Dr Robin Taylor (Cambridge Crystallographic Data Centre) for a search and analysis of N–H···N interactions on the Cambridge Structural Database.

References

1 See, P. Jutzi, *Adv. Organomet. Chem.*, 1986, **26**, 217; J. W. Connoly and A. Hoff, *Adv. Organomet. Chem.*, 1981, **19**, 123; M. A. Beswick, J. S. Palmer and D. S. Wright, *Chem. Soc. Rev.*, 1998, **27**, 225.

2 See, M. A. Beswick, C. N. Harmer, P. R. Raithby, A. Steiner, K. L. Verhorevoort and D. S. Wright, *J. Chem. Soc., Dalton Trans.*, 1997, 2029 and refs. therein.

3 K. Jonas, *Angew. Chem.*, 1985, **97**, 292; *Angew. Chem., Int. Ed. Engl.*, 1985, **24**, 295.

4 M. A. Beswick, C. Brasse, M. A. Halcrow, P. R. Raithby, C. A. Russell, A. Steiner, R. Snaith and D. S. Wright, *J. Chem. Soc., Dalton Trans.*, 1996, 3793; P. R. Raithby, M.-A. Rennie, C. A. Russell, A. Steiner and D. S. Wright, *Organometallics*, 1996, **15**, 639.

5 D. Stalke, M. A. Paver and D. S. Wright, *Angew Chem., Int. Ed. Engl.*, 1993, **32**, 428; A. J. Edwards, M. A. Paver, Paul R. Raithby, C. A. Russell, D. Stalke, A. Steiner and D. S. Wright, *J. Chem. Soc., Dalton Trans.*, 1993, 1465; M. A. Paver, C. A. Russell, D. Stalke and D. S. Wright, *J. Chem. Soc., Chem. Commun.*, 1993, 1349; A. J. Edwards, M. A. Paver, P. R. Raithby, C. A. Russell and D. S. Wright, *J. Chem. Soc., Chem. Commun.*, 1993, 1086; A. J. Edwards, M. A. Paver, P. R. Raithby, C. A. Russell, A. Steiner, D. Stalke and D. S. Wright, *Inorg. Chem.*, 1994, **33**, 2370; M. A. Beswick, M. K. Davies, P. R. Raithby, A. Steiner and D. S. Wright, *J. Chem. Soc., Chem. Commun.*, 1996, 1619; M. A. Beswick, M. K. Davies, P. R. Raithby, A. Steiner and D. S. Wright, *Organometallics*, 1997, **16**, 1109; M. A. Beswick, C. A. Harmer, M. A. Paver, P. R. Raithby, A. Steiner and D. S. Wright, *Inorg. Chem.*, 1997, **36**, 1740; D. R. Armstrong, D. Moncrieff, C. A. Russell, D. Stalke and D. S. Wright, *Organometallics.*, 1997, **16**, 3340.

6 R. E. Allan, M. A. Beswick, M. K. Davies, P. R. Raithby, A. Steiner and D. S. Wright, *J. Organomet. Chem.*, 1998, **550**, 1.

7 See for example, S. E. Kabir, M. M. Karim, S. M. B. Ullah and K. I. Hardcastle, *J. Organomet. Chem.*, 1996, **517**, 155; J. A. Castro, J. Romero, J. A. Carcia-Vazquez, A. Castiñeiras and A. Sousa, *Polyhedron*, 1995, **14**, 2841.

8 The abreviations A–A and D–D are normally used to describe species with hydrogen bond acceptors and donor functionalities aligned parallel to each other so that these can act together to the same molecule. The difference here is that these functionalities are antiparallel in the units of **1** and **2**.

9 L. Pauling, *The Nature of the Chemical Bond*, Cornell University Press, Ithica, 3rd edn., 1960.
10 W. C. Hamilton and J. A. Ibers, *Hydrogen Bonding in Solids*, W. A. Benjamin, New York, 1968; J. Emsley, *Chem. Soc. Rev.*, 1980, **9**, 91.
11 Several examples of metal complexes containing doubly protonated TMEDA exist, for example, J. F. Darr, S. R. Drake, M. B. Hursthouse, K. M. Abdul Malik, S. A. S. Miller and D. M. P. Mingos, *J. Chem. Soc., Dalton Trans.*, 1997, 945; G. M. Kapteijn, D. M. Grove, W. J. J. Smeets, H. Kooijman, A. L. Spek and G. van Koten, *Inorg. Chem.*, 1996, **35**, 534.
12 The shortest hydrogen bond of this type occurs between imidazole and imidazolium.
13 J.-M. Lehn, *Angew. Chem.*, 1988, **100**, 91; *Angew. Chem., Int. Ed. Engl.*, 1988, **27**, 89.
14 A. D. Burrows, C.-W. Chan, C. M. Chowdhry, J. E. McGrady and D. M. P. Mingos, *Chem. Soc. Rev.*, 1995, 329 and refs. therein.
15 A. D. Burrows, D. M. P. Mingos, A. J. P. White and D. J. Williams, *J. Chem. Soc., Chem. Commun.*, 1996, 97.
16 P. J. Bailey, R. O. Gould, C. N. Harmer, S. Pace, A. Steiner and D. S. Wright, *J. Chem. Soc., Chem. Commun.*, 1997, 1161.
17 For other metal complexes involving helical association, see R. S. Bartlett, M. M. Olmstead and P. P. Power, *Inorg. Chem.*, 1986, **25**, 1243; E. Hey and F. Weller, *J. Chem. Soc., Chem. Commun.*, 1988, 782; N. D. R. Barnett, R. E. Mulvey, W. Clegg and P. A. O'Neil, *J. Am. Chem. Soc.*, 1991, **113**, 8187; D. Philip and J. F. Stoddart, *Angew. Chem.*, 1996, **108**, 1242; *Angew. Chem., Int. Ed. Engl.*, 1996, **35**, 1154.
18 G. Wilkinson, F. A. Cotton and J. M. Birmingham, *J. Inorg. Nucl. Chem.*, 1956, **2**, 95.
19 D. Stalke and T. Kottke, *J. Appl. Crystallogr.*, 1993, **26**, 615.
20 PROCESS, A Program for Indexing and Processing R-AXIS II Imaging Plate Data, T. Higashi, Rigaku Corp., 1990.
21 TEXSAW, version 1.7-1, Molecular Structure Corporation, The Woodlands, TX, 1985, 1992, 1995; G. Altomore, G. Cascaraner, C. Gracarazzo, G. Guagliardi, M. C. Burla, G. Polidani and M. Camalli, *J. Appl. Crystallogr.*, 1994, **27**, 435.
22 G. M. Sheldrick, SHELXL 93, Program for Crystal Structure Refinement, University of Göttingen, 1993.

Paper 8/09066A